

# Building Integrated Photovoltaics/Thermal (BIPV/T) System: A New Dynamic Simulation Model and a Case Study

Andreas Athienitis – Concordia University – aathieni@encs.concordia.ca

Giovanni Barone – University of Naples Federico II – giovanni.barone@unina.it

Annamaria Buonomano – University of Naples Federico II – annamaria.buonomano@unina.it

Adolfo Palombo – University of Naples Federico II – adolfo.palombo@unina.it

## Abstract

In this paper, the energy performance of a façade open loop Building Integrated Photovoltaic/Thermal (BIPV/T) system with air as working thermal fluid is investigated. For this aim a new dynamic simulation model based on a detailed transient finite difference thermal network is developed. For a complete building energy performance analysis, such model was implemented in a suitable computer tool written in MatLab (called DETECT 2.3, suitably modified). The presented simulation model includes a parametric analysis tool useful to minimize the building energy demand.

In order to show the potential of the developed code, a comprehensive case study related to a multi-floor office building located in several climate zones is developed. In particular, with the aim to identify the design and operating parameters minimizing the overall energy consumptions, while guaranteeing the comfort of occupants, a suitable optimization procedure is carried out. Results show that through the produced electricity and thermal energy it is possible to balance the overall building energy demand approaching the NZEB goal.

## 1. Introduction

BIPV/T systems represent an innovative and effective measure for achieving net-zero energy buildings. Using this innovative technology, electricity and useful heat are simultaneously produced by solar energy. Therefore, the reduced building energy consumption is obtained by also boosting the share of renewables, as required for reaching the nearly-zero energy building target (Yang and Athienitis, 2016).

In order to carry out feasibility analysis as well as for the best design of such BIPV/T system, the use of

suitable energy performance simulation tool is recommended. Different numerical approaches can be followed and are commonly used by researchers. Specifically, the performance of the BIPV/T system are analysed through the use or development of one or two dimensional thermal network models (based on finite-difference schemes), through the modified Hottel-Whillier model or computational fluid dynamics (CFD) techniques (Yang and Athienitis, 2016). The active and passive energy performance of BIPV/T systems can also be assessed by using commercial software such as TRNSYS, EES, etc. (Lamnatou et al., 2015). Yet, in terms of energy, thermal, optical simulations, the available literature highlights the need of more studies focusing on the building and on the building/system configuration (Lamnatou et al., 2015). In addition, for suitable consideration of critical design and operating details, often neglected in commercial tools, novel mathematical models are being developed (Rounis et al., 2016). In this context, with the aim at investigating the BIPV/T performance, by taking into account both passive and active effects, this paper presents a new in-house developed simulation model for the dynamic analysis of BIPV/T systems. In particular, it refers to opaque photovoltaic panels integrated in the building skin façade or roof with air as working thermal fluid (Fig. 1).

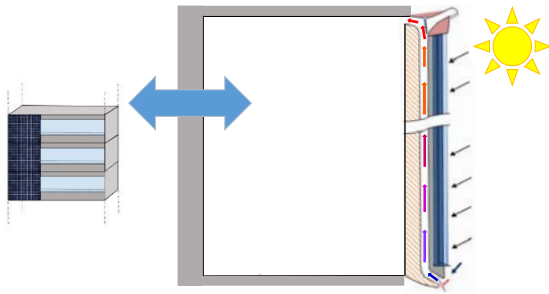


Fig. 1 – Modelled façade BIPV/T system

The developed model is implemented in a suitable computer tool, suitably modified for the simulation of BIPV/T system. The model is written in MatLab, called DETECt 2.3, validated through a recognised code-to-code procedure (Buonomano et al., 2016), and allows performing complete building energy performance analyses (Buonomano and Palombo, 2014). Particular attention is paid to:

- assessing the system energy fluxes, temperatures and airflow distribution into the BIPV/T system (air gap included);
- obtaining dynamic energy performance results also referred to the BIPV/T system active effects (e.g., space heating through the air heated by the BIPV/T system, increased electricity production efficiency by the outdoor air flow, increased coefficient of performance of heat pumps) and passive ones (winter free heating and summer overheating through BIPV/T wall heat transfer);
- achieving optimal design and operating parameters for minimizing the building energy demand (by simultaneously guaranteeing the hygrothermal comfort). Such outcomes can be easily calculated through a single simulation run (through a suitable optimization tool implemented in the presented computer code);
- assessing economic and environmental impact performance indexes of the system as a function of climate, building envelope features and use.

The developed model is particularly suitable for the simulation of the thermal behaviour of multi-zone and multi-floor buildings, with facades/roofs partially or totally integrated with PV/T. Helpful results for the process of BIPV/T systems design and feasibility analysis in case of new or retrofitted buildings can be also obtained (Buonomano et al.,

2016). Furthermore, for comparison purposes, additional dynamic simulation models related to conventional building-plant systems are also implemented in the code.

In order to show the capability of the code and the potential of BIPV/T systems, four different case studies were developed. They refer to a multi-floor office building located in four different weather zones: Freiburg (South-Germany); Bolzano (North-Italy); Naples (South-Italy); Almeria (South-Spain).

## 2. Simulation Model

In this section, the developed dynamic simulation model for the performance analysis of the above-mentioned innovative BIPV/T system is described. The model, written in MatLab, is embedded in a new release, appropriately modified, of DETECt 2.3, a tool for the whole building energy, economic and environmental performance analysis (Buonomano and Palombo, 2014). Dynamic building-plant system performance results can be assessed starting by building envelope features, design and operating BIPV/T parameters, hourly climate data.

The mathematical model of BIPV/T system is based on a finite volume approach. A set of explicit equations is obtained for each node of the adopted thermal resistance capacitance (RC) network, including conductive, radiative, and convective heat transfer occurring within and through the BIPV/T system. A sketch of the considered BIPV/T system thermal network adopted to model the system behaviour is shown in Fig. 2. Here, 2-D transient heat transfer is simultaneously taken into account in: PV panels; air flow gap between PV panels and the back plates; back wall integrated with the BIPV/T. 1-D transient heat transfer is taken into account between the BIPV/T system and the outdoor and the indoor environment. In the following, the description of the mathematical models relative to the BIPV/T system, including the integrating wall, is reported; all model details related to the heat transfer phenomena taking place within the building interior zone are reported in Buonomano and Palombo (2014). In order to calculate the gradient of the air temperature within the BIPV/T cavity, each element of the system (i.e. PV, air gap channel, back plate) is subdivided, along the vertical

direction, in  $N$  equal control volumes (e.g., strips). The same assumption is considered for the perimeter wall integrating with the PV/T. However, different from the PV and back plate, for the wall integrating the PV/T,  $N$  capacitive nodes are modelled according to the occurring thermal mass. Note that building indoor / outdoor air temperature gradients are neglected.

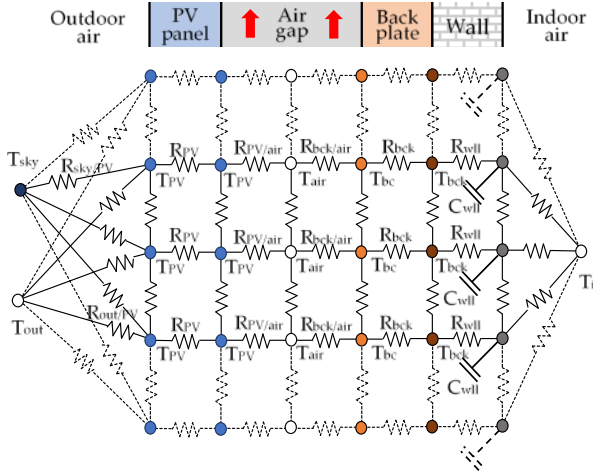


Fig. 2 – BIPV/T system RC thermal network

In order to solve the modelled thermal network for the BIPV/T system and to calculate each nodal temperature, an explicit finite difference method is used. In each time step interval  $[(t + 1) - t]$  and for each  $i$ -th PV node, the discretised differential equation describing the energy rate of change is:

$$(\rho c V)_{PV} (T_{PV(i)}^{(t+1)} - T_{PV(i)}^{(t)}) = \sum_{n=i-1}^{i+1} \frac{(T_{PV(n)}^{(t)} - T_{PV(i)}^{(t)})}{R_{PV,PV}^{cond}} \Delta \vartheta + \dot{Q}_{sol,PV} + \left[ \frac{(T_{out}^{(t)} - T_{PV(i)}^{(t)})}{R_{out,PV}^{conv}} + \frac{(T_{sky}^{(t)} - T_{PV(i)}^{(t)})}{R_{sky,PV}^{rad}} + \frac{(T_{air}^{(t)} - T_{PV(i)}^{(t)})}{R_{cavity,PV}^{conv}} + \frac{(T_{bc}^{(t)} - T_{PV(i)}^{(t)})}{R_{bc,PV}^{rad}} \right] \Delta \vartheta \quad (1)$$

where  $T$  is the temperature of the  $i$ -th PV node;  $Q_{sol,PV}$  is the incident solar radiation on PV;  $R_{m,PV}$  are the thermal resistances between the  $i$ -th node of the PV panel and other neighbours components (Fig. 2).  $R_{m,PV}^{cond}$ ,  $R_{m,PV}^{conv}$  and  $R_{m,PV}^{rad}$  are, respectively, conductive, convective and radiative thermal resistances. Note that, in Equation (1) the temperature of  $i$ -th PV panel layer is the unknown variable.

The differential equation describing the energy rate of change of each control volume linked to the  $i$ -th air temperature node is:

$$L \cdot \bar{h}_{c,cavity} (T_{PV(i)}^{(t)} - T_{air(i)}^{(t)}) + L \cdot \bar{h}_{c,cavity} (T_{bc(i)}^{(t)} - T_{air(i)}^{(t)}) = \dot{m}_{air} c_{p,air} \frac{dT}{dz} \quad (2)$$

According to previous studies, in the developed model an exponential profile is taken into account for simulating the air temperature in the ventilated gap of the BIPV/T system (Pantic et al., 2014):

$$T_{(z)air} = T_{(in)air} \cdot e^{\left( \frac{2\bar{h}_{c,cavity}Lz}{\dot{m}_{air} c_{p,air}} \right)} + \left( \frac{\bar{h}_{c,cavity} T_{PV(i)}^{(t)} + \bar{h}_{c,cavity} T_{bc(i)}^{(t)}}{2\bar{h}_{c,cavity}} \right) \left( 1 - e^{\left( \frac{2\bar{h}_{c,cavity}Lz}{\dot{m}_{air} c_{p,air}} \right)} \right) \quad (3)$$

The heat transfer coefficient inside the cavity,  $\bar{h}_{c,cavity}$  is approximated by an experimental linear correlation, which is a function of the air velocity (Chen et al., 2010). The following correlation, recommended for design purposes, is:

$$\bar{h}_{c,cavity} = 3.94 \cdot v_{air} + 5.45 \quad (4)$$

In each  $t$ -th time step and for each  $i$ -th back plate layer node, the same approach used for PV layers is used. Thus, the discretised differential equation describing the energy rate change for each temperature node of the back plate is:

$$(\rho c V)_{bc} (T_{bc(i)}^{(\tau+1)} - T_{bc(i)}^{(\tau)}) = \sum_{n=i-1}^{i+1} \frac{(T_{bc(n)}^{(\tau)} - T_{bc(i)}^{(\tau)})}{R_{bc,bc}^{cond}} \Delta \vartheta + \left[ \frac{(T_{wall}^{(\tau)} - T_{bc(i)}^{(\tau)})}{R_{wall,bc}^{cond}} + \frac{(T_{air}^{(\tau)} - T_{bc(i)}^{(\tau)})}{R_{cavity,bc}^{conv}} + \frac{(T_{PV}^{(\tau)} - T_{bc(i)}^{(\tau)})}{R_{PV,bc}^{rad}} \right] \Delta \vartheta \quad (5)$$

where  $R_{m,bc}^{cond}$ ,  $R_{m,bc}^{conv}$  and  $R_{m,bc}^{rad}$  are respectively a conductive, convective and radiative thermal resistance due to the interaction between the system back-plate and others building elements. Note that in Fig. 2, the back-plate nodes are linked to the wall capacitive nodes that are subsequently linked to the indoor air temperature node  $T_{in}$ .

The discretised differential equation for each  $i$ -th façade layer describing the energy rate of change of each façade temperature node (wall in Fig. 2) is:

$$(\rho c V)_{fac} (T_{fac(i)}^{(t+1)} - T_{fac(i)}^{(t)}) = \sum_{n=i-1}^{i+1} \frac{(T_{fac(n)}^{(t)} - T_{fac(i)}^{(t)})}{R_{fac,fac}^{cond}} \Delta \vartheta + \left[ \frac{(T_{in}^{(t)} - T_{fac(i)}^{(t)})}{R_{ind,fac}^{conv} + R_{fac,fac}^{cond}} + \frac{(T_{out}^{(t)} - T_{fac(i)}^{(t)})}{R_{out,wall}^{conv} + R_{fac,fac}^{cond}} \right] \Delta \vartheta + \dot{Q}_{sol,fac} \quad (6)$$

where  $T$  is the temperature of the  $i$ -th façade node and  $Q_{sol,PV}$  is the solar radiation incident on the building façade.

Within the thermal zone, the calculation of the indoor air temperature  $T_{in}$ , as well as of the interior wall comprising the thermal zone is carried out by following the mathematical approach embedded in DETECT (Buonomano and Palombo, 2014). In particular, the discretized differential equation on the indoor air node is:

$$C_{in} \frac{dT_{in}}{dt} = \sum_{n=1}^N \frac{T_n^{(t)} - T_{in}^{(t)}}{R_{n,PVTwall}^{conv}} + \sum_{p=1}^P \frac{T_p^{(t)} - T_{in}^{(t)}}{R_{p,wrf}^{conv}} + \dots + Q_g^{(t)} + Q_v^{(t)} + Q_{HVAC}^{(t)} \quad (7)$$

where  $C_{in}$  is the thermal capacitance of the zone indoor air, whose temperature,  $T_{in}$ , is assumed as homogeneous in the space. The heat exchange between the  $2 \times N$  internal surfaces nodes of the wall integrating the PV/T (*wll*) and the indoor air one is proportional to the internal convective resistances,  $R_{n,PVTwall}^{conv}$ , calculated as a function of the surfaces condition (e.g., ascendant or descendant flow, wall inclination); similarly the heat exchange between the  $P$  internal surfaces nodes of the interior building elements (walls, roof, and floor (*wrf*)) and the indoor air one is proportional to internal convective resistances,  $R_{p,wrf}^{conv}$ . In addition, with the exception of the radiative thermal load, all the sensible heat gains are networked to the indoor air node only (as purely convective). They are:  $Q_g$  is the internal gains due the occupants, lighting and electrical appliances;  $Q_v$  is the ventilation thermal load (including both the infiltration and ventilation terms);  $Q_{HVAC}$  is the sensible heat to be supplied to or to be removed from the building space by an ideal heating and cooling system (necessary to maintain the indoor air at the desired set point temperatures). Details about the assessment and handling of the solar radiation within the zone, and on calculation of the long-wave radiation exchange on the internal surfaces are available in (Buonomano and Palombo, 2014). The gross electricity power production is obtained by:

$$P_{el} = \eta_{PV} \cdot Q_n \cdot A_n \quad (8)$$

where  $\eta_{pv}$  is the PV efficiency, assumed linearly decreasing with the increasing operating temperature, taken from Pantic et al. (2010). Note that the

solar radiation incident on the PV modules, operating at their maximum power point condition, is assumed as uniform.

Finally, by the presented code it is possible to take into account the heat recovered through the PV/T channel on the heating energy consumptions. Specifically, such thermal energy can be directly supplied, as free heating, to the air thermal zone or supplied to the evaporator of a heat pump to increase its performances. To this aim, for the assessment of the coefficient of performance of air-to-air, as well as air-to-water heat pump/chiller ( $COP_{HVAC,heat}$  and  $COP_{HVAC,cool}$ ), it is possible to follow two methods within the code: i) a manufacturers data look up approach and ii) recommended analytical equations. In both methods, COPs are calculated by means of the nominal values (given by constructors) and as a function of the occurring operating conditions and the part-load ratio  $f_{PLR}$ .

### 3. Case Studies

The developed case studies refer to a ten-floor building (East–West oriented longitudinal axis) for open office spaces. In particular, the simulation is referred to a singular South facing perimeter thermal zone. On its South-façade a BIPV/T system and a window (4-6-4 air filled double-glazed system) of 10 m<sup>2</sup> are modelled (Fig. 3).

The thicknesses of building walls (U-value = 1.30 W/(m<sup>2</sup> K)) and floor/ceiling (U-value = 1.10 W/(m<sup>2</sup> K)) are 30 and 25 cm respectively. The wall layers include hollow bricks ( $\lambda = 0.33$  W/(m K),  $\rho = 1600$  kg/m<sup>3</sup>,  $c = 1200$  J/(kg K)) and thermal insulation ( $\lambda = 0.05$  W/(m K),  $\rho = 13.0$  kg/m<sup>3</sup>,  $c = 1100$  J/(kg K)). The direct solar radiation transferred through the windows to the inside zone is assumed to be absorbed by the floor and the interior walls with absorption factor of 0.4 and 0.2, respectively. For such zone, a ventilation rate equal to 1 Vol/h and a crowding index of 0.12 person/m<sup>2</sup> are taken into account. The interior thermal loads include people (95 W/p at 26 °C, varying with  $T_{in}$ ), lighting, and equipment (9 W/m<sup>2</sup>). Interior walls are modelled as adiabatic. The simulation starts on 0:00 of January 1 and ends at 24:00 of December 31. Both the

innovative and traditional simulated buildings are heated/cooled through a 10 kW air-to-air electric heat pump/chiller. The HVAC system is switched on from 08:00 to 20:00 (week days only).

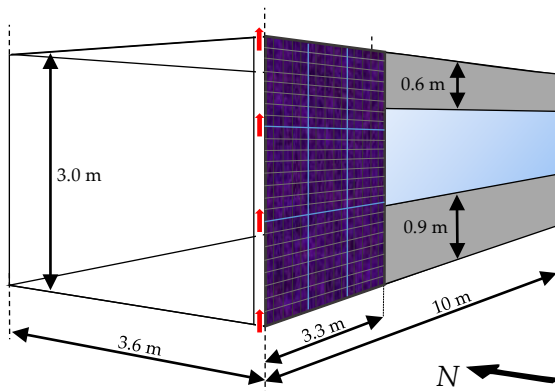


Fig. 3 – Perimeter zone of one sample building floor

The heating and cooling set points are 20 and 26 °C. The simulations were carried out through DETECT 2.3 and refer to 4 different weather zones, Table 1. Here, heating and cooling degree days (HDD and CDD), incident solar radiation (ISR) and the considered heating and cooling periods are also reported.

Table 1 – Climatic zones, climatic indexes and system scheduling

	HDD Kd	CDD Kd	ISR kWh/m <sup>2</sup> y	Heating	Cooling
Freiburg	3110	253	1114	No limitations	
Bolzano	2641	475	1251	10/15 - 4/15	6/01 - 9/30
Naples	1479	727	1529	11/15 - 3/31	6/01 - 9/30
Almeria	783	961	1724	12/01 - 3/31	6/01 - 9/30

For the innovative system layout, the BIPV/T system outlet air is exploited in the winter to supply the evaporator of the adopted air-to-air heat pump for space heating. A minimum gap air flow rate of 0.1 m<sup>3</sup>/s is obtained through a fan. If the natural convection allows higher flow rates the fan is switched off. In this case study, the potential direct free heating (for  $T_{inlet} > 20$  °C) is neglected. The BIPV/T system air flow enhances the PV efficiency.

## 4. Results and Discussion

In Fig. 4 for the weather zone of Naples, the time

histories of the indoor air temperature at the 9<sup>th</sup> floor for both the innovative and traditional building layouts are reported for two sample winter and summer days (January 10–11 and June 29–30, respectively). Here, it possible to observe that during the hours in which the HVAC system is switched on, the setpoint temperatures are always reached. During night time, the passive effect of BIPV/T can be easily observed: the free floating indoor air temperature increases due to the heat gain due to the thermal inertia of the wall integrating the PV/T. In particular, during the winter season the resulting free floating temperatures approaches the setpoint better than the ones obtained in the traditional building, whereas the contrary occurs in the summer.

The BIPV/T system passive effect can be also observed in Fig. 5. Here, for Naples, the calculated sensible thermal loads ( $Q_{HVAC}$ ) profiles detected on the 9<sup>th</sup> building floor are depicted for the same time hours of Fig. 4, for both the innovative and traditional building configurations. During the heating season a reduction of the thermal loads vs. the traditional building (Fig. 4, top) is obtained through the BIPV/T system passive effects (space free heating). Note that in this case study the winter BIPV/T system active effect is the enhanced heat pump efficiency obtained by exploiting the heat extraction through the solar collectors. Conversely, during the summer HVAC running, an increase of cooling loads is obtained through the passive effect (space overheating) due to the BIPV/T system adoption (Fig. 4, bottom).

For a winter sample day (January 10), in Fig. 6 the temperature profiles of the PV panels and of the related gap air are reported vs. the length of the BIPV/T system gap (building height) and of the time hours (Fig. 6). Note that, the gap air temperatures follow and approach the PV panels ones (ranging between 35 and 52 °C), which obviously depends on the solar irradiation incident on the solar collector surface. The maximum temperature increase detected between the outlet and inlet air is about 20 °C (therefore, the temperature gain achieved per building floor is about equal to 2 °C). Note that, such air temperature growth is due to the slow air velocity (minimum level set at 0.45 m/s). During summer an overheating of the gap air temperatures

can be observed (mostly in hot summer climates). In this case, an increase of the gap air fan speed is recommended. It is noteworthy to observe that the calculated nighttime temperature of the PV can be lower than that of the traditional building envelope and of the outdoor air.

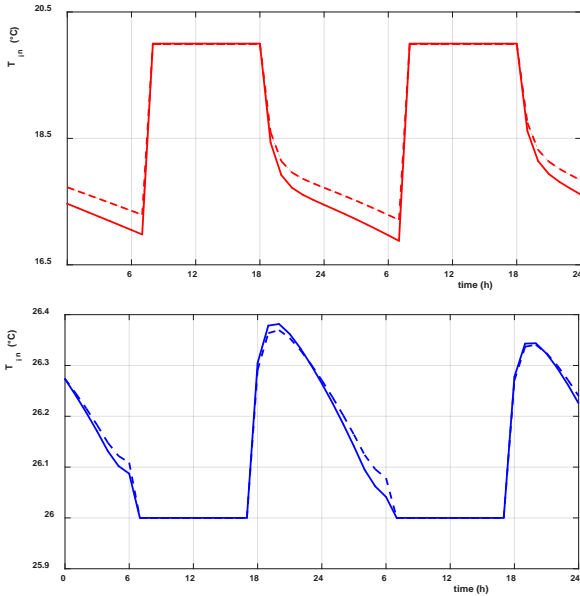


Fig. 4 – Indoor air temperatures in January 10 and 11 (up) and June 29 and 30 (down). Dashed lines: BIPV/T system layout. Solid lines: traditional building

This result is due to the long-wave infrared radiative heat exchange between the building external surfaces and the sky.

In Fig. 7 for the weather zone of Naples the temperature profile of the BIPV/T panels, gap air, and outdoor air are reported as a function of the length of the BIPV/T system gap for a sample winter time instant (January 10 at 13:00). In this figure, it can be observed that the gap air temperature reaches the selected indoor air setpoint (20 °C) at a building height corresponding to the 4<sup>th</sup> floor (12 m). Note that such occurrence is related to an inlet outdoor air temperature of 12 °C. By Fig. 6 and 7 it can be also observed that the PV panels are suitably cooled by the air flowing in the gap (an increased PV efficiency is achieved). Simultaneously, the outdoor air is gradually heated along the BIPV/T gap (the obtained thermal energy is usefully recovered). A decreasing difference trend of such temperatures can be observed in Fig. 7.

In Fig. 8, for the weather zone of Naples, the calculated monthly heating and cooling demands, are shown for both the innovative and conventional building. It is possible to observe the month-by-month effects of the BIPV/T system on the building energy requirement.

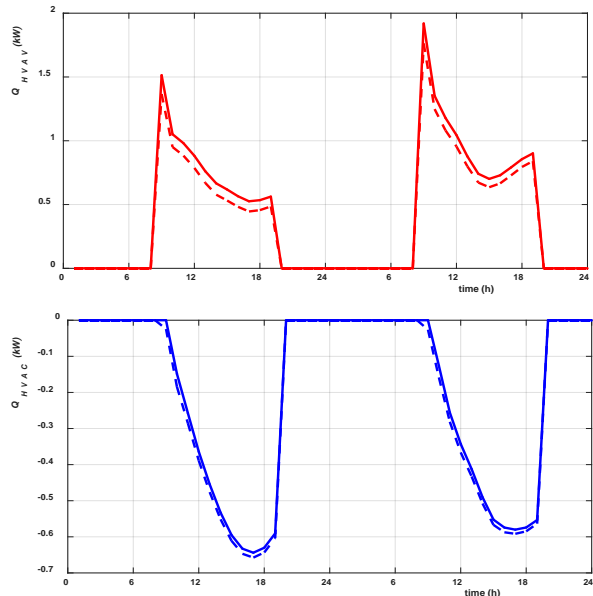


Fig. 5 – Sensible thermal loads ( $Q_{HVAC}$ ) in January 10 and 11 (up) and June 29 and 30 (down). Dashed lines: BIPV/T system layout. Solid lines: traditional building

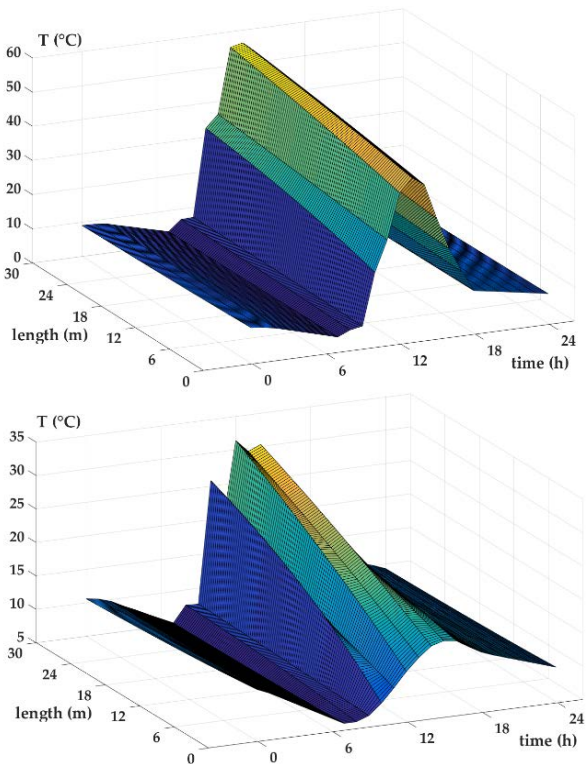


Fig. 6 – Temperatures of BIPV/T collectors (up) and gap air (down) in January 10

In Table 2 for all the investigated weather zones the yearly heating and cooling demands of the traditional and the innovative system are reported for 3 sample floors and the whole building.

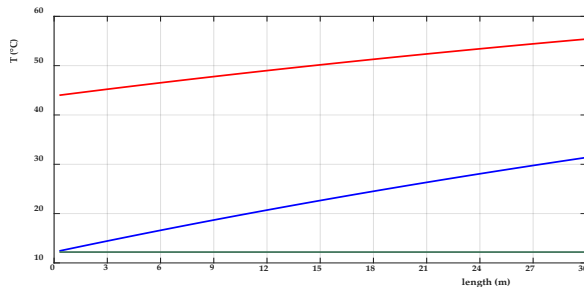


Fig. 7 - Temperatures of the BIPV/T panel (red line), gap air (blue line) and outdoor air (green line) for January 10 at 13:00

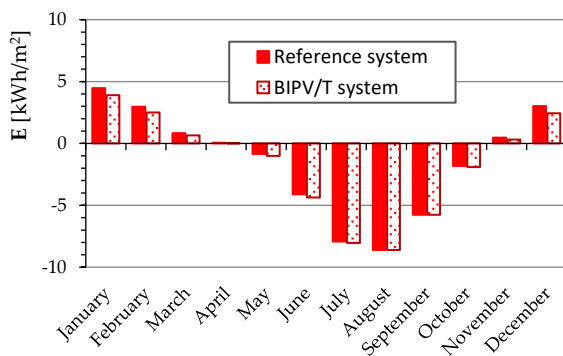


Fig. 8 – Monthly heating and cooling demands

Table 2 – Reference and BIPV/T system: energy demand for heating (H) and cooling (C) expressed as [kWh/m<sup>2</sup>y]

Reference system		Freiburg	Bolzano	Naples	Almeria
Floor 1 <sup>st</sup>	H	58.6	47.1	11.8	0.3
	C	-5.6	-16.4	-29.0	-34.6
Floor 5 <sup>th</sup>	H	58.6	47.1	11.8	0.3
	C	-5.6	-16.4	-29.1	-34.7
Floor 10 <sup>th</sup>	H	58.7	47.1	11.8	0.3
	C	-5.6	-16.4	-29.1	-34.7
Building [MWh/y]	H	21.1	17.0	4.2	0.11
	C	-2.0	-5.9	-10.5	-12.5
BIPV/T system		Freiburg	Bolzano	Naples	Almeria
Floor 1 <sup>st</sup>	H	53.5	43.3	10.2	0.2
	C	-5.9	-16.6	-28.8	-34.4
Floor 5 <sup>th</sup>	H	53.0	42.8	9.8	0.2
	C	-6.2	-17.1	-29.6	-35.2
Floor 10 <sup>th</sup>	H	52.5	42.2	9.5	0.2
	C	-6.5	-17.7	-30.5	-36.0
Building [MWh/y]	H	19.1	15.4	3.5	0.07
	C	-2.2	-6.2	-10.7	-12.7

The obtained results vary as a function of the building floor height, due to the different corresponding temperatures of the BIPV/T system wall. In general, the building heating energy savings are higher than

the increase of the cooling demands. Obviously, heating and cooling demands are strongly dependent on the weather conditions. In Table 3 the yearly electricity production calculated for all the weather zones is reported. Note that the production efficiency is enhanced through the cooling air flowing in the BIPV/T system gap. Table 3 shows that higher productions are achieved at lower building floors (i.e. stronger heat extraction potential causes lower cooling air temperatures, Fig. 7). Of course, larger electricity productions are obtained where the ISR is higher.

Table 3 – BIPV/T system: electricity production

	Freiburg	Bolzano	Naples	Almeria
Floor 1 <sup>st</sup>	29.0	34.7	37.5	41.1
Floor 5 <sup>th</sup> [kWh/y]	28.8	34.5	37.2	40.8
Floor 10 <sup>th</sup>	28.6	34.3	37.0	40.5
Building [MWh/y]	10.4	12.4	13.4	14.7

In Table 4 the yearly final electricity uses calculated for all the investigated weather zones are reported. The calculated results include the PV production and the electricity consumption of the electric heat pump/chiller, gap air fan, lighting and machineries. Here, the influence of the building floors height results to be very weak. It is noteworthy to observe that, for all the case studies the adoption of the BIPV/T system allows to reach the nearly or net zero energy building target.

Table 4 – Final electricity use expressed as [kWh<sub>e</sub>/(m<sup>2</sup>y)]

		Freiburg	Bolzano	Naples	Almeria
Floor 1 <sup>st</sup>	Ref.	54.5	52.2	39.5	36.8
	BIPV/T	26.3	18.3	2.4	-4.4
Floor 5 <sup>th</sup>	Ref.	54.5	52.2	39.5	36.8
	BIPV/T	26.4	18.4	2.8	-3.9
Floor 10 <sup>th</sup>	Ref.	54.5	52.2	39.6	36.8
	BIPV/T	26.4	18.6	3.1	-3.5
Building [MWh <sub>e</sub> /y]	Ref.	19.6	18.8	14.2	13.2
	BIPV/T	9.5	6.6	1.0	-1.4
[y]	SPB	8.2	6.8	6.3	6.0

In fact, in addition to the building self-consumption fulfilment an electricity export can be achieved. The best results are obtained in Almeria, with an electricity export of 1.4 MWh<sub>e</sub>/y. By such results a swift and simplified economic feasibility analysis can be carried out by taking into account an incentive of 50 % on the system capital cost and an electricity purchase and feed-in tariff of 0.18 and 0.08 €/kWh<sub>e</sub>, respectively. In particular, satisfactory

paybacks are achieved, Table 4. In Table 5 the yearly primary energy saving and avoided overall CO<sub>2</sub> emission for all the investigated weather zones are reported. An average primary energy factor of 0.46 kWh<sub>e</sub>/kWh<sub>p</sub> and an average CO<sub>2</sub> conversion factor of 0.423 kg<sub>CO2</sub>/kWh<sub>e</sub> are considered. Remarkable primary energy savings are obtained. Note that results lower than zero (Almeria) suggest energy exports (innovative building). Interesting results are also obtained in terms of avoided CO<sub>2</sub>, confirming (besides the economic convenience), the overall feasibility of such technology.

Table 5 – Primary energy savings expressed as [kWh<sub>p</sub>/m<sup>2</sup>y] and avoided CO<sub>2</sub> emissions

		Freiburg	Bolzano	Naples	Almeria
Floor 1 <sup>st</sup>	Ref.	118.4	113.4	85.8	80.0
	BIPV/T	57.2	39.8	5.3	-9.5
Floor 5 <sup>th</sup>	Ref.	118.5	113.5	85.9	80.0
	BIPV/T	57.3	40.1	6.1	-8.6
Floor 10 <sup>th</sup>	Ref.	118.5	113.5	86.1	80.0
	BIPV/T	57.4	40.3	6.8	-7.6
Building [MWh <sub>p</sub> /y]	Ref.	42.6	40.9	30.9	28.8
	BIPV/T	20.6	14.4	2.2	-3.1
[tCO <sub>2</sub> /y]	ΔCO <sub>2</sub>	4.3	5.1	5.6	6.2

## 5. Conclusion

In this paper, a new dynamic simulation model for the energy performance assessment of façade building integrated photovoltaic/thermal (BIPV/T) systems is presented. For a complete building energy performance analysis, such model was implemented in a computer tool written in MatLab (called DETECT 2.3). The developed model takes into account both the active and passive BIPV/T system effects. The active effects pertain to the efficiency increase through the air flowing in the system gap of both the PV panels and the electric heat pump for space heating.

In order to show the potentiality of the presented tool a suitable case study is developed. It refers to an office building located in four different weather zones. Here, a BIPV/T façade is suitably designed for electricity and thermal energy productions. Simulations show interesting benefits vs. traditional buildings in terms of energy efficiency, economic savings, system payback, and avoided CO<sub>2</sub> emissions. As evidenced by the results, useful design

and operating data are achieved for reaching the nearly or net zero energy building goal for both new and renovated buildings.

## Nomenclature

### Symbols

$\dot{m}$	flow rate (kg/s)
$Q$	thermal load (W)
$R$	thermal resistance (K/W)
$T$	temperature (K)

### Subscripts/Superscripts

<i>air</i>	air-gap air
<i>bck</i>	back-plate
<i>faç</i>	façade
<i>in</i>	indoor air
<i>out</i>	outdoor air
<i>PV</i>	photovoltaics panel

## References

- Buonomano, A., G. De Luca, U. Montanaro, A. Palombo. 2016. "Innovative technologies for NZEBs: An energy and economic analysis tool and a case study of a non-residential building for the Mediterranean climate". *Energy and Buildings* 121: 318-343. doi: 10.1016/j.enbuild.2015.08.037.
- Buonomano, A., A. Palombo. 2014. "Building energy performance analysis by an in-house developed dynamic simulation code: An investigation for different case studies". *Applied Energy* 113: 788-807. doi: 10.1016/j.apenergy.2013.08.004.
- Chen, Y., K. Galal, A.K. Athienitis. 2010. "Modeling, design and thermal performance of a BIPV/T system thermally coupled with a ventilated concrete slab in a low energy solar house: Part 2, ventilated concrete slab". *Solar Energy* 84(11): 1908-1919. doi: 10.1016/j.solener.2010.06.012.
- Lamnatou, C., J.D. Mondol, D. Chemisana, C. Maurer. 2015. "Modelling and simulation of Building-Integrated solar thermal systems: Behaviour of the coupled building/system configuration". *Renewable and Sustainable Energy Reviews* 48: 178-191. doi: 10.1016/j.rser.2015.03.075.

- Pantic, S., L. Candanedo, A.K. Athienitis. 2010. "Modeling of energy performance of a house with three configurations of building-integrated photovoltaic/thermal systems". *Energy and Buildings* 42(10): 1779-1789. doi: 10.1016/j.enbuild.2010.05.014.
- Rounis, E.D., A.K. Athienitis, T. Stathopoulos. 2016. "Multiple-inlet Building Integrated Photovoltaic/Thermal system modelling under varying wind and temperature conditions". *Solar Energy* 139: 157-170. doi: 10.1016/j.solener.2016.09.023.
- Yang, T., A.K. Athienitis. 2016. "A review of research and developments of building-integrated photovoltaic/thermal (BIPV/T) systems". *Renewable and Sustainable Energy Reviews* 66: 886-912. doi: 10.1016/j.rser.2016.07.011.